ORIGINAL PAPER

Inhibitive action of Clematis gouriana extract on the corrosion of mild steel in acidic medium

**Gopiraman Mayakrishnan · Sakunthala Pitchai ·
Kanmani Raman · Alex Ramani Vincent ·
Sulochana Nagarajan**

Abstract The inhibitive action of Clematis gouriana (CG) on mild steel (MS) corrosion in 1.0 M HCl solution was studied. Inhibition efficiency of CG was carried out by using various weight loss methods, potentiodynamic polarisation, and electrochemical impedance spectroscopy. Inhibition efficiencies of up to 95.70% for CG can be obtained. Adsorption of CG on the MS surface was found to obey the Langmuir adsorption isotherm. Free energy of adsorption calculated from the temperature studies revealed the possibility of both chemisorptions and physisorption. The adsorbed film on the MS surface containing the CG inhibitor was also characterized by Fourier transform infrared spectroscopy (FTIR) and scanning electron microscope and energy-dispersive spectrum. The possible active ingredient responsible for the anticorrosion effect is identified as aporphine alkaloid which is isolated and screened for the anticorrosion effect using electrochemical studies. The possible mode of corrosion inhibition of aporphine alkaloid is also derived using FTIR studies.

Keywords Clematis gouriana (CG) · Corrosion inhibitor · Polarisation · Adsorption isotherm · Electrochemical impedance spectroscopy (EIS) · SEM–EDS

G. Mayakrishnan · S. Nagarajan (✉)
Department of Chemistry, National Institute of Technology,
Trichy 620015, India
e-mail: n.sulocha@gmail.com

S. Pitchai · K. Raman · A. R. Vincent
Department of Chemistry, St. Joseph's College,
Trichy 620002, India

G. Mayakrishnan
Nano Fusion Technology Research Lab, Faculty of Textile
Science and Technology, Shinshu University,
Ueda City, Nagano 386–8567, Japan

Introduction

Acid solutions are widely used for industrial cleaning, oil well acidification and in the petrochemical processes. Hydrochloric acid is generally used in the pickling processes of metals and alloys. The corrosion of steel in such environments and its inhibition constitute a complex problem of processes. Using inhibitors is one of the most practical methods for protection of metals against corrosion, especially in acidic media.

Organic compounds containing electronegative functional groups and π electron in triple or conjugated double bonds are usually good inhibitors. Heteroatoms such as sulphur, phosphorus, nitrogen and oxygen as well as aromatic rings in their structure are the major adsorption centres [1, 2].

The recent trend is toward environment friendly inhibitors. As most of the natural products are nontoxic, biodegradable, readily available and in plenty, various parts—seeds, fruits, leaves, flowers, etc.—have been used as corrosion inhibitors [3].

A large number of scientific studies have been devoted to the inhibitive action of some plant extracts on the corrosion of mild steel (MS) in acidic medium, showing that these extracts could serve as good corrosion inhibitors; the reported extracts include Justicia gendarussa [4], Lawsonia inermis [5], Occimum viridis, Telferia occidentalis, Azadirachta indica, Hibiscus sabdariffa and Garcinia kola, Phyllanthus amarus [6], Olea europaea L., Ferula harmonis, Chamaemelum mixtum L., Cymbopogon proximus, Nigella sativa L. and Phaseolus vulgaris L. [7], Zanthoxylum alatum [8], Piper nigrum, Mentha pulegium [9] and Lupinus albus L. [10].

Clematis gouriana belongs to the family of hairy climbers of Ranuncluaceae. The aim of the present work is to develop a naturally occurring, cheap and environmentally safe inhibitor for the corrosion of MS.
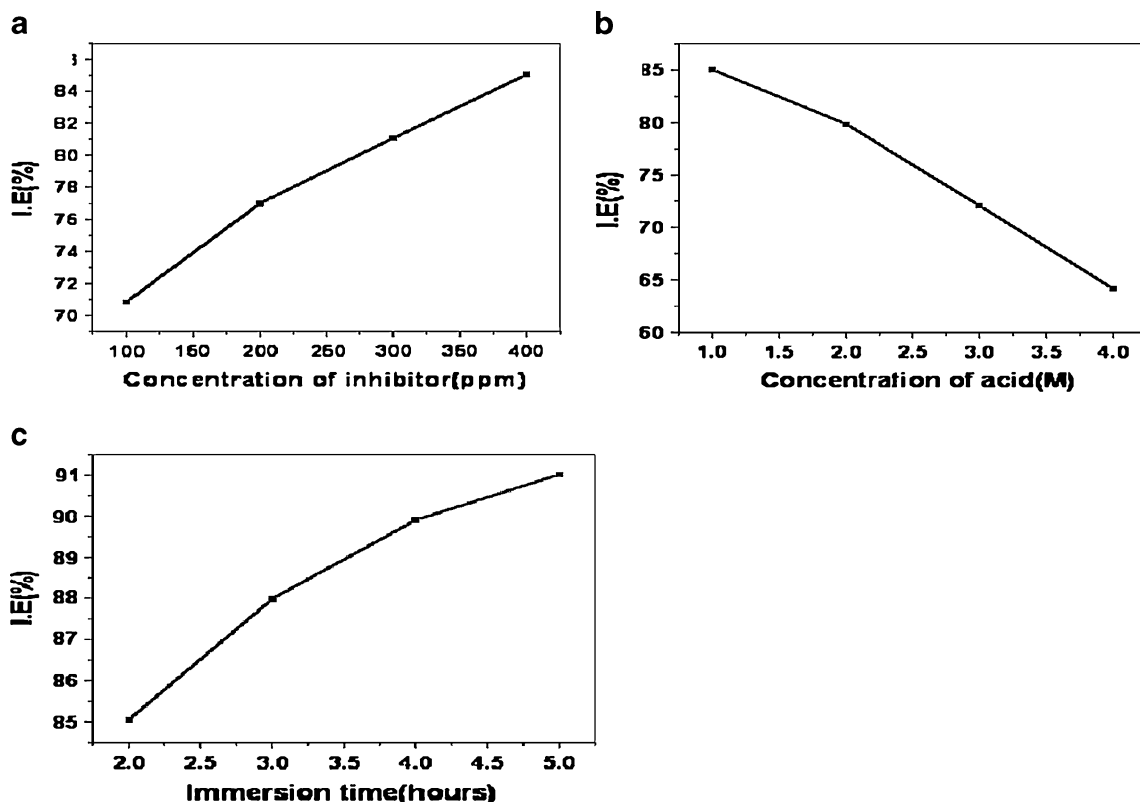
a

b

c

Fig. 1 Variation of inhibition efficiency with different **a** inhibitor concentrations, **b** acid concentrations, and **c** immersion time

In the present study, the inhibition potential of the ethanolic extract of *C. gouriana* in 1.0 M HCl using weight loss, electrochemical, adsorption isotherms, Fourier transform infrared (FTIR) spectroscopy and scanning electron microscopy energy-dispersive X-ray spectroscopy (SEM–EDS) techniques have been investigated. The plant *C. gouriana* was used for the treatment of infection, inflammation, skin disorders and rheumatic pain, for alleviating pain and as an antitoxic agent. The plant of *C. gouriana* contains magnofluorine, aporphine alkaloid [11] and protoanemonin [12].
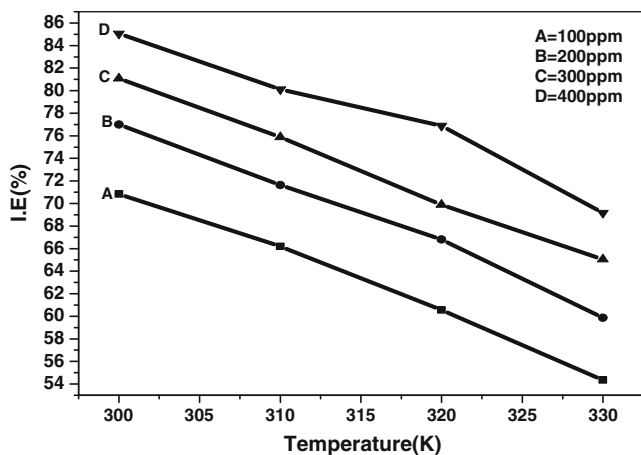
Experimental

Inhibitor preparation

Fresh leaves (2 kg) of *C. gouriana* were collected at Maruthamalai of Coimbatore district in Tamil Nadu, India, and extracted with ethanol (5×500 mL). The alcoholic
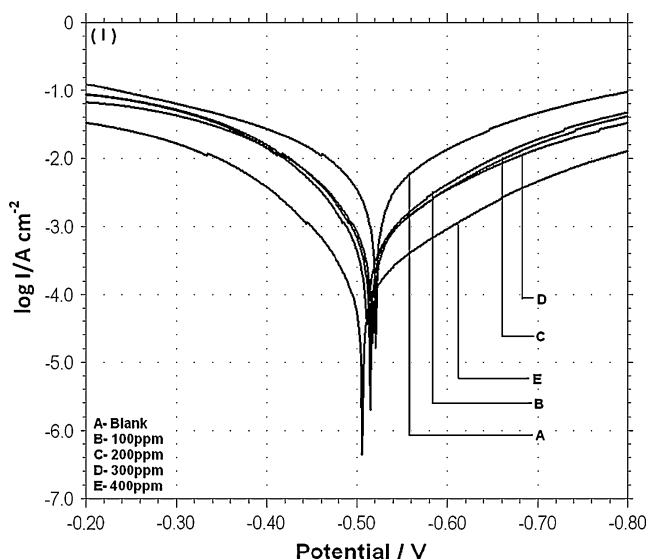

Fig. 2 Variation of inhibition efficiency with different temperatures

Fig. 3 Electrochemical impedance spectrum for MS in 1.0 M HCl with and without inhibitor

Table 1 Tafel polarisation parameter values for the corrosion of MS in 1.0 M HCl in the presence and absence of inhibitor

Concentration of inhibitor (ppm)	I_{corr} (µA cm^{-2})	E_{corr} (mV vs. SCE)	b_{c} (mV/decade)	b_{a} (mV/decade)	I.E. (%)
0 (Blank)	1,559	−528	5.67	6.00	–
100	90	−518	6.45	6.84	94.23
200	84	−508	6.80	6.94	94.61
300	73	−509	6.21	6.46	95.31
400	67	−502	5.98	6.18	95.70

extract was concentrated in vacuo and left in an ice chest for a few days, and various concentrations of the solid plant extract of *C. gouriana* (inhibitor) were prepared by dissolving the known quantity of the resultant powder in the acid medium.

Specimen preparation

MS specimens containing C=0.10%, Mn=0.34%, Cr=0.22% and Fe=99.34% were used for the study. MS specimens of size 2.5×2.0×0.06 cm were used for the weight loss study, specimens with an exposed area of 1 cm^2 were used for electrochemical study and 191 cm was used for SEM–EDS analysis. The surface preparation of mechanically polished specimens was carried out using different grades of emery paper and then degreased with acetone.

Electrochemical studies

CH electrochemical analyzer model 604B was used to record the Tafel polarisation curve and Nyquist impedance curve. A conventional three-electrode system was used for this purpose. An MS specimen of an exposed area of 1 cm^2 was used as a working electrode. Pt and SCE were used as auxiliary and reference electrodes, respectively. The working electrode was polished with 1/0-, 2/0-, 3/0- and 4/0-grade emery papers and degreased with double-distilled water and acetone before usage. The linear Tafel segments of the anodic and cathodic curves were extrapolated to the corrosion potential to obtain the corrosion current densities. Inhibition values were calculated from the i_{corr} values. And the anodic and cathodic polarisation curves were recorded by the potential range from −0.85 to −0.15 mV and scan rate of 0.01 mV/s.

AC impedance measurements were carried out at E_{corr} immersion on standing in the atmosphere of air at the range from 1 to 10,000 Hz at an amplitude of 10 mV. The impedance diagrams are given by Nyquist representation.

FTIR

The MS specimen was coated with inhibitors with suitable solvent, and it was kept for 24 h to evaporate the solvent. The surface film was scraped carefully, and its FTIR spectra were recorded using a PerkinElmer FTIR instrument.

SEM and EDS analysis

The specimens for surface morphological examination were immersed in an acid containing optimum concentration of inhibitors and blank for 2 h. Then, they were removed, rinsed quickly with acetone and dried. The analysis was performed on a Hitachi S 3,000 H scanning electron microscope.
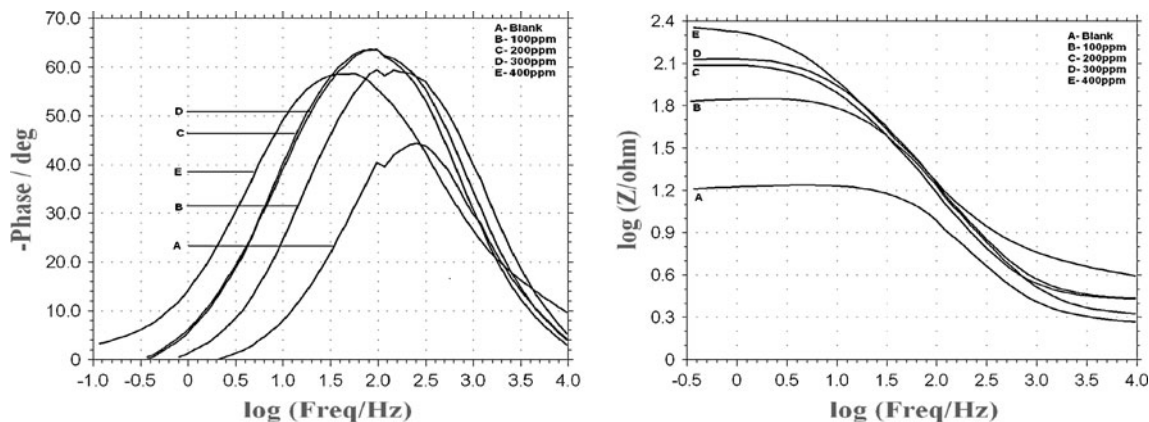

Fig. 4 Nyquist plots for MS in 1.0 M HCl without and with various concentrations of inhibitor

Concentration of inhibitor (ppm)	R_{ct} (Ω cm^2)	C_{dl} (μF cm^{-2})	I.E. (%)
0 (Blank)	16.19	196.70	–
100	60.23	94.4	73.12
200	107.69	29.6	84.97
300	118.61	26.9	86.35
400	223.99	7.90	92.77

Results and discussion

Weight loss study

The weight loss experiments were performed at 300, 310, 320 and 330 K with different concentrations of inhibitor. The optimized immersion time is 2 h. After weighing accurately, three parallel specimens were completely immersed in an open beaker containing 250 mL 1.0 M HCl without and with different concentrations of CG at 300 K. After 2 h, the specimens were taken out, washed, dried and weighed accurately. The inhibition efficiency (I.E.) is calculated as follows:

$$I.E.(\%) = \frac{W_0 - W}{W_0} \times 100 \tag{1}$$

where, W_0 and W are the values of average weight loss without and with inhibitor, respectively.

Temperature study was carried out at 300, 310, 320 and 330 K for 2 h time duration in 1.0 M HCl solution. From the weight loss method, the I.E. was calculated. The standard free energy of adsorption ($\Delta G°_{ads}$) at different temperatures was calculated using the following equation:

$$\Delta G°_{ads} = -RTIn(55.5K) \tag{2}$$

And K is given by

$$K = \frac{\theta}{1 - \theta} \times \frac{1}{C} \tag{3}$$

where θ is the degree of coverage on the metal surface, C is the concentration in parts per million and K is the equilibrium constant. The degree of surface coverage (θ) for optimum concentration of inhibitor in 1.0 M HCl at 300–330 K for 2 h of immersion time has been evaluated from the weight loss values. A plot of log ($\theta/1-\theta$) versus $1/T$ gave a straight line. The values of enthalpy of activation

(ΔH) and entropy of activation (ΔS) were calculated using the following equation:

$$Rate = \frac{RT}{Nh} \exp\frac{\Delta S}{R} \exp\frac{-\Delta H}{RT} \tag{4}$$

where h is Planck's constant; N, the Avogadro number and R, the gas constant. A plot of log (CR/T) versus $1/T$ gave a straight line with a slope of ($-\Delta H/2.303R$) and an intercept of [(log(R/Nh)+($\Delta S/2.303R$)].

The values of percentage inhibition efficiency (percent I. E.) obtained from weight loss measurements for MS at different concentrations of inhibitor in 1.0 M HCl at 300 K are shown in Fig. 1a. It was observed that the inhibitors inhibit the corrosion of MS in HCl solution, at all concentrations used in the study, i.e. 100–400 ppm.

From Fig. 1a, it is clear that the addition of the inhibitor increased the inhibition efficiency in the acid medium through the adsorption of the basic constituents of *C. gouriana* on the MS surface and provides protection against corrosion [13]. It is clear that the inhibitor shows maximum inhibition of 85.05% at 400 ppm concentration.

From Fig. 1b, it is clear that the inhibition efficiency of the inhibitor was at 400 ppm concentration in different acid concentrations. It is evident from the values that an increase in concentration of acid decreases the inhibition efficiency
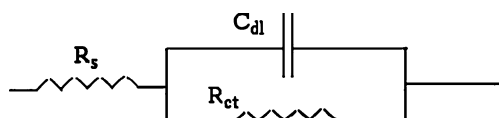
Fig. 5 Bode plots for mild steel in 1.0 M HCl in the presence and absence of different concentrations of inhibitor
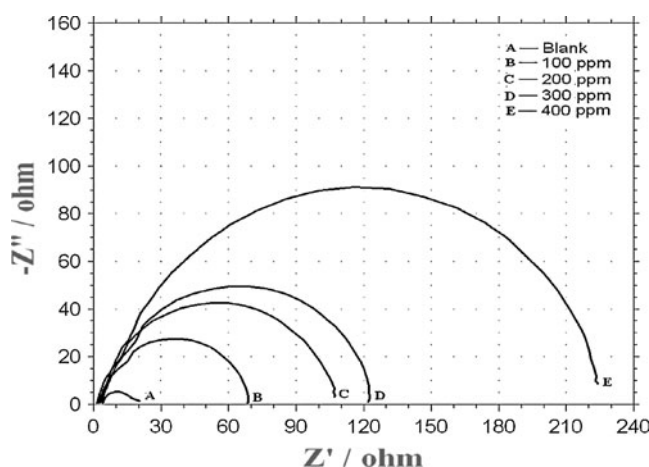
Fig. 6 The equivalent circuit model for electrochemical impedance measurements
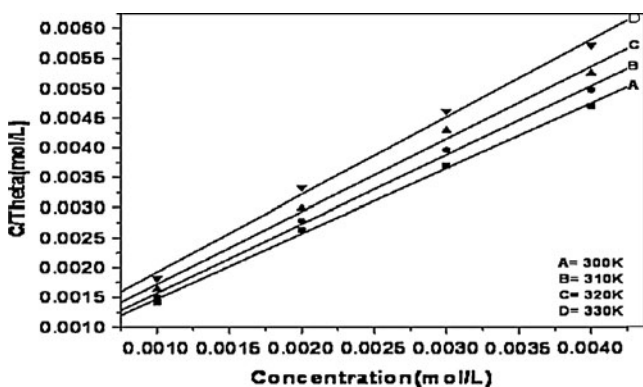
Fig. 7 Langmuir plot for the inhibitor on MS in 1.0 M HCl at different temperatures

of the inhibitor. This is due to the aggressiveness of the acid solution.

From Fig. 1c, it is clear that the inhibition efficiency of the inhibitor was at 400 ppm concentration in 1.0 M HCl with different immersion time. It is very clear from Fig. 1b that, when the immersion time increases, the inhibition efficiency is also increased. This is due to stability and persistence of the adsorbed inhibitor layer on the metal surface. It is noted that the inhibitor shows maximum efficiency in 5 h of immersion.

Inhibition efficiencies of the inhibitor of 400 ppm concentration at different temperatures are shown by Fig. 2. It is observed from Fig. 2 that, with an increase in the temperature, the inhibition efficiency decreases. The inhibitor shows maximum inhibition efficiency at 300 K. This gave a clue that the mechanism of adsorption of the inhibitor may be due to physisorption, because the physisorption is due to weak van der Waal's forces, which disappear at elevated temperatures.

Tafel polarisation

Figure 3 shows the cathodic and anodic polarisation plots of mild steel immersed in 1.0 M HCl at 300 K in the absence and presence of different concentrations of inhibitor. Electrochemical parameters such as corrosion potential (E_{corr}), cathodic and anodic Tafel slopes (b_c and b_a) and corrosion current density (i_{corr}) were extracted by Tafel extrapolating the anodic and cathodic lines and are listed in

Table 3. The percentage of inhibition efficiency was calculated using the following equations:

$$I.E.~(\%) = \frac{(I'_{corr} - I_{corr})}{I'_{corr}} \times 100 \qquad (5)$$

where I'_{corr} and I_{corr} are corrosion current densities in the absence and presence of inhibitor. From the results in Table 1, it can be observed that the values of corrosion current density (I_{corr}) of MS in the inhibitor-containing solutions were lower than those for the inhibitor-free solution. The polarisation curves (Fig. 3) show that this inhibitor has an effect on both the cathodic and anodic slopes (b_c and b_a) and suppressed both cathodic and anodic processes. This indicates a modification of the mechanism of cathodic hydrogen evolution as well as anodic dissolution of iron, which suggests that the inhibitor powerfully inhibits the corrosion process of mild steel, and its ability as corrosion inhibitor is enhanced as its concentration is increased. The suppression of the cathodic process can be due to the covering of the surface with monolayer due to the adsorbed inhibitor. It can also be seen from Table 1 that the anodic Tafel slope b_a increases in the presence of the inhibitor. This observation may be ascribed to changes in the charge transfer coefficient for the anodic dissolution of Fe by virtue of the presence of an additional energy barrier due to the presence of adsorbed inhibitor. Further inspection of Table 1 reveals also that E_{corr} values do not show any significant change in the presence of various concentrations of the inhibitor suggesting that the inhibitor is a mixed type inhibitor in 1.0 M HCl; it influences both metal dissolution and hydrogen evolution.

Electrochemical impedance spectroscopy

The effect of inhibitor concentration on the impedance behaviour of MS in 1.0 M HCl solution at 300 K is presented in Fig. 4. The curves show a similar type of Nyquist plot for MS in the presence of various concentrations of inhibitor. As seen from Fig. 4, The Nyquist plots contain a depressed semi-circle, with the centre below the real X-axis, whose size is increased by increasing the inhibitor concentration, indicating that the corrosion is mainly a charge transfer process [14]. A loop is also seen at

Table 3 Thermodynamic parameters for MS in 1.0 M HCl in the absence and presence of the inhibitor at different temperatures

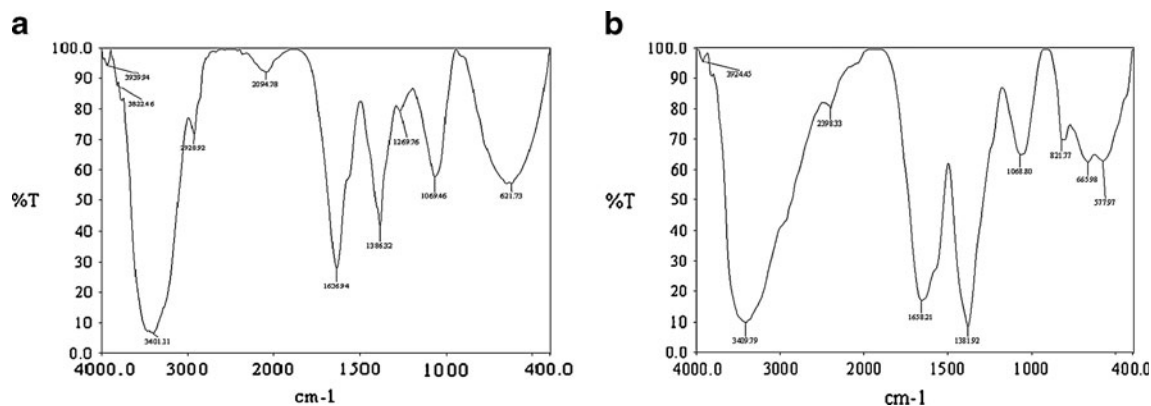| Temperature (K)	R^2	Slope	ΔG°_{ads} (kJ/mol)	K_{abs} (kJ/mol)	ΔH_{ads} (kJ/mol)	ΔS_{ads} (kJ/mol)
300	0.9990	1.091	−29.63	2.604	−41.31	−38.70
310	0.9987	1.154	−29.43	2.398	−41.31	−38.70
320	0.9971	1.213	−28.95	1.960	−41.31	−38.70
330	0.9974	1.304	−28.50	1.652	−41.31	−38.70

Fig. 8 a FTIR spectrum of the inhibitor b FTIR spectrum of the inhibitor adsorbed on the metal surface

low frequencies which could arise from the adsorbed intermediate products such as $(FeCl^-)ads$ in the absence of the inhibitor and/or $(FeCl^-Inh^+)ads$ in the presence of the inhibitor according to the mechanism proposed by Solmaz et al. [15], for the corrosion of MS in HCl solution. The depressed semi-circle is the characteristic of solid electrodes and often refers to frequency dispersion which arises due to the roughness and others in homogeneities of the surface. It is clear that the impedance response of MS is significantly changed after addition of the inhibitor. It is worth noting that the change in the concentration of the inhibitor did not alter the style of the impedance curves, suggesting a similar mechanism of inhibition is involved. The impedance parameters derived from these plots are given in Table 2. Moreover, the R_{ct} and C_{dl} values were computed from the Bode plot Fig. 5. The double layer capacitance (C_{dl}) and inhibition efficiency (I.E. percent) are calculated from the following equation:

Fig. 9 Mode of adsorption of the aporphine alkaloid on the MS surface in 1.0 M HCl medium

$$C_{dl} = \frac{1}{(2 \Pi f_{max} R_{ct})} \tag{6}$$

$$\text{I.E. (\%)} = \frac{(R'_{ct} - R_{ct})}{(R'_{ct})} \times 100 \tag{7}$$

where F_{max} is the frequency at apex on the Nyquist plot, R'_{ct} and R_{ct} are the charge transfer resistance values in the presence and absence of the inhibitor, respectively. As seen from Table 2, the R_{ct} values of inhibited substrates are increased with the concentration of the inhibitor. On the other hand, the values of C_{dl} are decreased with an increase in inhibitor concentration which is most probably due to the decrease in local dielectric constant and/or increase in thickness of the electrical double layer, suggesting that CG acts via adsorption at the metal/solution interface [16–18]. It could be assumed that the decrease of C_{dl} values is caused by the gradual replacement of water molecules by adsorption of organic molecules on the electrode surface, which decreases the extent of the metal dissolution [16]. For analysis of the impedance spectra containing one loop, the electrical equivalent circuit given in Fig. 6 was used. In the given electrical equivalent circuit, R_s is the solution resistance; R_{ct}, the charge transfer resistance, and C_{dl} is the double layer capacitance. I.E. was calculated from the charge transfer resistance (R_{ct}) values.

Adsorption isotherms

The mechanism of corrosion inhibition may be explained on the basis of adsorption behaviour. The degrees of surface coverage (θ) for different inhibitor concentrations were evaluated by weight loss data. Data were tested graphically by fitting to various isotherms. It is observed that the plot obeys Langmuir adsorption isotherms through surface coverage of adsorbed inhibitor on the MS surface, and
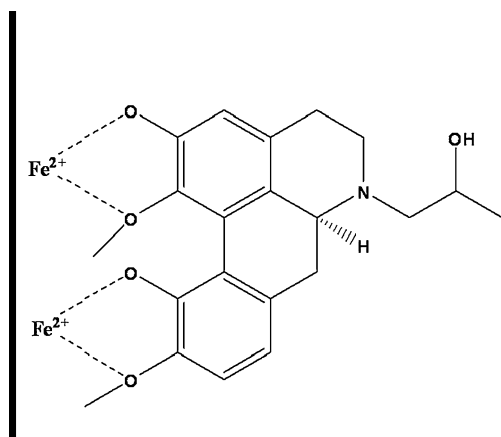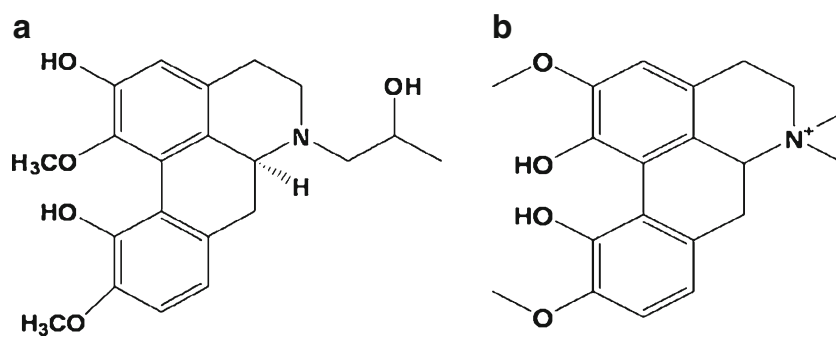
Fig. 10 Chemical structures of **a** aporphine alkaloid and **b** magnoflorine

consequently, there is no interaction between the inhibitor adsorbed at the metal surface. The higher inhibitive property of the inhibitor is attributed to the presence of π electrons in oxygen and the larger molecular size, which ensures greater coverage of the metallic surface.

Figure 7 shows the Langmuir isotherm. In the case of plant extract *C. gouriana* shows expected linear relationship is well approximated in Langmuir isotherm (correlation coefficient R^2 equals 0.9990), and the line has a slope of 1.091 at 300 K. The deviation of the slope from unity is often interpreted as a sign that the adsorbing species occupy more or less than a typical adsorption site at the metal/solution interface.

Adsorption of the inhibitor occurs because of the interaction energy between the inhibitor and the metal surface. Basic information on the interaction between the inhibitor and the surface of MS can be provided by adsorption isotherm. A correlation between surface coverage (θ) defined and the concentration of inhibitor (C_{inh}) in electrolyte can be represented by the Langmuir adsorption isotherm.

Surface coverage values (θ) for the inhibitor were obtained from the weight loss measurements for various concentrations at different temperatures (300–330 K), as shown in Table 3. The best-fitted straight line is obtained for the plot of C_{inh}/θ versus C_{inh} with slopes around unity in both the cases. The correlation coefficient (R^2) was used to choose the isotherm that best fits experimental data. This suggests that the adsorption of the inhibitor on the metal surface followed the Langmuir adsorption isotherm (Fig. 7).

From the intercepts of the straight lines C_{inh}/θ-axis, K values were calculated and are given in Table 3. The most important thermodynamic adsorption parameters are the free energy of adsorption (ΔG°_{ads}). The adsorption constant, K_{ads}, is related to the standard free energy of adsorption, ΔG°_{ads}, with the equation (Eq. 1).

The negative values of G_{ads} indicate the stability of the adsorbed layer on the steel surface and spontaneity of the adsorption process. The dependence of ΔG°_{ads} on temperature can be explained by two cases as follows:

(a) ΔG°_{ads} may increase (becomes less negative) with the increase of temperature which indicates the occurrence of exothermic process.

(b) ΔG°_{ads} may decrease (becomes more negative) with increasing temperature indicating the occurrence of endothermic process.

Generally, the magnitude of ΔG°_{ads} around −20 kJ/mol or less negative is assumed for electrostatic interactions that exist between inhibitor and the charged metal surface (i.e. physisorption). Those around −40 kJ/mol or more negative are indicating charge sharing or transferring from organic species to the metal surface to form a coordinate type of metal bond (i.e. chemisorptions) [16, 19, 20].

Thermodynamic parameter values of free energy of adsorption (ΔG°_{ads}) with temperature reveal that the inhibition of MS by inhibitor is an endothermic process. The free energy of adsorption (ΔG°_{ads}) for *C. gouriana* is around −29 kJ/mol. So, it provides evidence for both physisorption and chemisorption [21, 22]. Adsorption
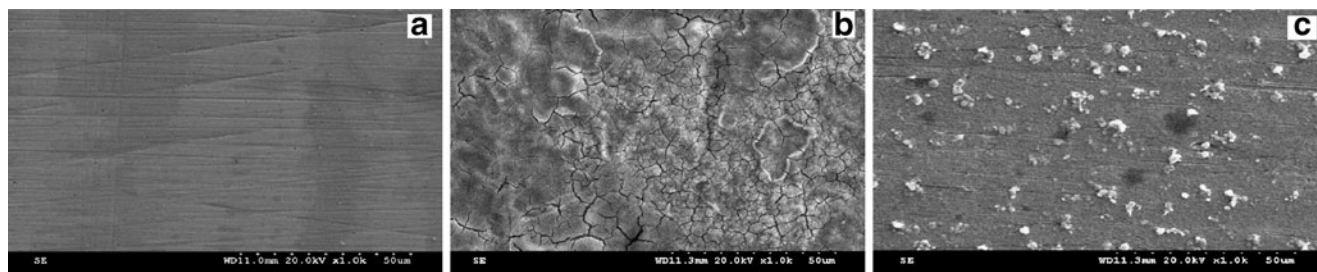

Fig. 11 SEM images of **a** polished MS plate, **b** MS in 1.0 M HCl and **c** MS in 1.0 M HCl (with inhibitor)
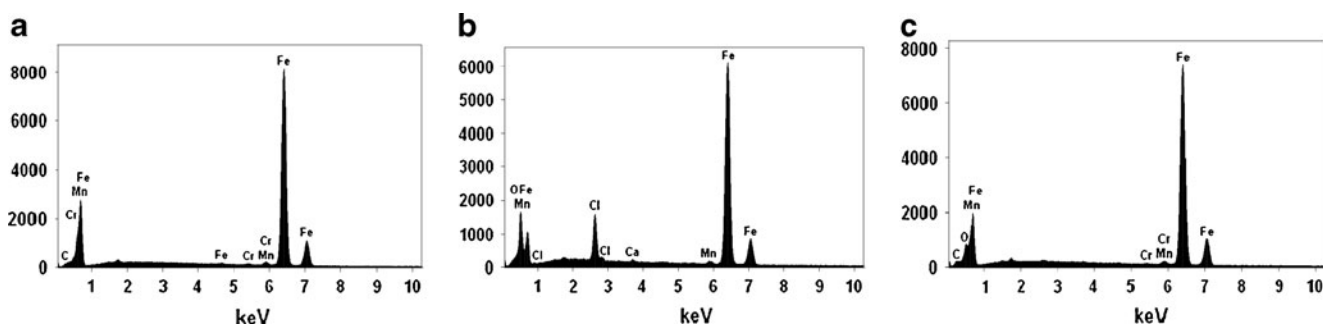
Fig. 12 EDS images of the **a** MS, **b** MS in 1.0 M HCl and **c** MS in presence of inhibitor

process can occur by electrostatic forces between ionic charges or dipoles of the adsorbed species and the electric charge on the metal surface. The negative value of ΔS_{ads} reflects the exothermic nature of the adsorption process on steel. Also, the inhibitor can be adsorbed onto the metal surface via the electron transfer from the adsorbed species to the vacant electron orbital of low energy in the metal to form a coordinate type of link. Therefore, the inhibitor is absorbed on the metal surface, thereby increasing the effectiveness of the corrosion inhibitor.

FTIR spectrum

The FTIR spectra taken for the characterization of both pure aporphine alkaloid and the corrosion product are displayed in Fig. 8a and b. FTIR spectroscopy of aporphine alkaloid is shown in Fig. 8a. The strong broad band at 3,401 cm^{-1} is attributed to O–H stretching. The band at 2,928 cm^{-1} is related to C–H stretching vibration. The strong band at 1,636 cm^{-1} is assigned to C=C stretching vibration. Besides these, the absorption bands at 1,069 cm^{-1} can be assigned to the C–O–C stretching vibration. The absorption bands below 1,000 cm^{-1} are assigned to the C–H bending vibrations.

Spectrum (8a) shows all the characteristic bands corresponding to the functional groups present in aporphine alkaloid, and (8b) shows the scratched film formed over the MS surface in 1.0 M HCl. In Fig. 8b, broadening of the O–H band at 3,409 cm^{-1} and C–O–C band at 1,068 cm^{-1} suggests that the aporphine alkaloid makes a coordination bond with the metal surface through the above-said heterocyclic centres which are shown in Fig. 9 [23]. The

magnetic moments for the PCB–Fe^{2+} complex have been measured at room temperature, and the μ_{eff} value was 0 BM. It reveals that Fe was in +2 oxidation state.

Explanation for inhibition

CG is composed of numerous naturally occurring organic compounds. The inhibitive action of CG toward the acid corrosion of steel can be attributed to the adsorption of its components onto the steel surface. The important constituents of the extract are aporphine alkaloid and magnoflorine, and the chemical structures are shown in Fig. 10. The FTIR result also shows that CG contains oxygen and nitrogen atoms in functional groups (O–H, C–N, C=C, C–O–C) and an aromatic ring, which meets the general consideration of typical corrosion inhibitors. CG might be protonated in the acid medium as follows:

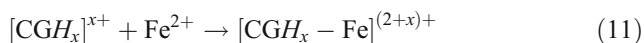$$CG + xH^+ \leftrightarrow [CGH_x]^{x+} \qquad (8)$$

Thus, in aqueous acidic solutions, CG exists either as neutral molecules or in the form of cations (protonated CG). In general, two modes of adsorption could be considered. The neutral CG may adsorb on the metal surface via the chemisorption mechanism, involving the displacement of water molecules from the metal surface and the sharing of electrons between the oxygen atom and Fe. CG can also adsorb on the metal surface on the basis of donor–acceptor interactions between p electrons of the aromatic ring and vacant d orbitals of Fe. On the other hand, it is well known that the steel surface charges positive charge in acid solution, so it is difficult for the protonated

Table 4 EDS analysis result of MS and MS in 1.0 M HCl in the absence and presence of inhibitor

Medium	Composition					
	Fe	O	C	Cl	Mn	Cr
MS (a)	99.34	–	0.10	–	0.34	0.22
Blank (b)	76.73	15.83	–	7.12	0.32	–
Clematis gouriana (c)	84.07	3.06	12.40	–	0.29	0.18

CG to approach the positively charged steel surface (H_3O^+/ metal interface) due to the electrostatic repulsion. Since chloride ions have a smaller degree of hydration, being specifically adsorbed, they create an excess negative charge toward the solution and favour more adsorption of the cations [24]; the protonated CG may adsorb through electrostatic interactions between the positively charged molecules and the negatively charged metal surface. In other words, there may be a synergism between Cl^- and CG, which improves the inhibitive capability of the inhibitor. When protonated, CG is adsorbed on the metal surface; a coordinate bond may be formed by partial transference of electrons from polar atoms (N and O atoms) to the metal surface. In addition, owing to lone-pair electrons of N and O atoms in CG, CG or protonated CG may combine with freshly generated Fe^{2+} ions on the steel surface forming metal inhibitor complexes:

$$Fe \rightarrow Fe^{2+} + 2e \tag{9}$$

$$CG + Fe^{2+} \rightarrow [CG - Fe]^{2+} \tag{10}$$

$$[CGH_x]^{x+} + Fe^{2+} \rightarrow [CGH_x - Fe]^{(2+x)+} \tag{11}$$

These complexes might get adsorbed onto the steel surface by van der Waals force to form a protective film to keep MS from corrosion. This assumption could be further confirmed by the FTIR results. SEM–EDS results prove that CG could adsorb onto the steel surface to form a denser and more tightly protective film. The film covers both anodic and cathodic reactive sites on the steel surface and inhibits both reactions at the same time.

SEM and EDS analysis

The scanning electron microscope images were recorded (Fig. 11) to establish the interaction of organic molecules with the metal surface. Fig. 11a indicates the finely polished characteristic surface of MS and shows some scratches which had arisen during polishing. Fig. 11b revealed that the immersed specimens were highly damaged in the presence of 1.0 M HCl, due to the direct attack of aggressive acids.

Figure 11c shows the formation of a protective film by plant extracts of *C. gouriana* on the metal surface which inhibits the corrosion significantly in acid medium. The micrographs (Fig. 11c) also showed the scratches formed during metal polishing were also covered well by the inhibitor. Hence, the inhibitors protect MS in 1.0 M HCl solution.

In the EDS spectrum of Fig. 12, it can be concluded that the MS surface corroded in aggressive medium has clearly

high chloride concentration compared to the surface in the presence of the inhibitor which was given in Table 4 [25].

Conclusions

The main conclusions drawn from these studies are:

1. By increasing the inhibitor concentration, the inhibition efficiency increases. At the concentration of 400 ppm, the plant extract has showed maximum inhibition efficiency of 95.70%.
2. Both polarisation studies and impedance measurements confirm the inhibiting nature of the inhibitor.
3. Tafel parameters give an idea that the inhibitor is mixed type in nature.
4. FTIR was recorded for the scrapped sample which showed a broad peak at coordination site frequencies which was bonded to iron.
5. The SEM image was taken for blank (1.0 M HCl) corroded and inhibitor plates. The surface of the blank plate has crevices, but the inhibitor surface was smooth.
6. Adsorption isotherms, Langmuir, provide evidence for both physisorption and chemisorption. Then, the thermodynamic parameter reveals that the adsorption process of inhibitors was spontaneous.
7. As a final point, the plant extracts of CG are good for HCl corrosion of MS.

References

1. Oguzie EE (2005) Corrosion inhibition of mild steel in hydrochloric acid solution by methylene blue dye. Mater Lett 59:1076–1079
2. Noor EA (2005) The inhibition of mild steel corrosion in phosphoric acid solutions by some N-heterocyclic compounds in the salt form. Corros Sci 47:33–55
3. Etre AYE, Abdullah M, Tantawy ZEE (2005) Corrosion inhibition of some metals using lawsonia extract. Corros Sci 47:385–395
4. Satapathy AK, Gunasekaran G, Sahoo SC, Amit K, Rodrigues PV (2009) Corrosion inhibition by *Justicia gendarussa* plant extract in hydrochloric acid solution. Corros Sci 51:2848–2856
5. Ostovari A, Hoseinieh SM, Peikari M, Shadizadeh SR, Hashemi SJ (2009) Corrosion inhibition of mild steel in 1 M HCl solution by henna extract. Corros Sci 51:1935–1949
6. Okafor PC, Ikpi ME, Uwaha IE, Ebenso EE, Ekpe UJ, Umoren SA (2008) Inhibitory action of *Phyllanthus amarus* extracts on the corrosion of mild steel in acidic media. Corros Sci 50:2310–2317
7. Abdel-Gaber AM, Abd-El-Nabey BA, Sidahmed IM, El-Zayady AM, Saadawy M (2006) Inhibitive action of some plant extracts on the corrosion of steel in acidic media. Corros Sci 48:2765–2779
8. Chauhan LR, Gunasekaran G (2007) Corrosion inhibition of mild steel by plant extract in dilute HCl medium. Corros Sci 49:1143–1161
9. Bouyanzer A, Hammouti B, Majidi L (2006) Pennyroyal oil from *Mentha pulegium* as corrosion inhibition of mild steel in 1 M HCl. Mater Lett 60:2840–2843

10. Abdel-Gaber AM, Abd-El-Nabey BA, Saadawy M (2009) The role of acid anion on the inhibition of the acidic corrosion of steel by lupine extract. Corros Sci 51:1038–1042

11. Raja Naika H, Krishna V (2008) Plant regeneration from callus culture of *Clematis gouriana* Roxb.—a rare medicinal plant. J Turk Biol 32:99–103

12. Southwell IA, Tucker DJ (1993) Protoanemonin in Australian *Clematis*. Phytochemisry 33:1099–1102, Umit

13. Ergun U, Yuzer D, Emregu KC (2008) The inhibitory effect of bis-2,6-(3,5-dimethylpyrazolyl)pyridine on the corrosion behaviour of mild steel in HCl solution. Mater Chem Phys 109:492–499

14. Bentiss F, Lagrenee M, Traisnel M, Hornez JC (1999) The corrosion inhibition of mild steel in acidic media by a new triazole derivative. Corros Sci 41:789–803

15. Solmaz R, Kardas G, Culha M, Yazici B, Erbil M (2008) Investigation of adsorption and inhibitive effect of 2-mercaptothiazoline on corrosion of mild steel in hydrochloric acid media. Electrochim Acta 53:5941–5952

16. Bentiss F, Lebrini M, Lagrenee M (2005) Thermodynamic characterization of metal dissolution and inhibitor adsorption processes in mild steel/2,5-bis(n-thienyl)-1,3,4-hiadiazoles/hydrochloric acid system. Corros Sci 47:2915–2931

17. Khaled KF (2003) The inhibition of benzimidazole derivatives on corrosion of iron in 1 M HCl solutions. Electrochim Acta 48:2493–2503

18. Behpour M, Ghoreishi SM, Soltani N, Salavati-Niasari M, Hamadanian M, Gandomi A (2008) Electrochemical and theoretical investigation on the corrosion inhibition of mild steel by thiosalicylaldehyde derivatives in hydrochloric acid solution. Corros Sci 50:2172–2181

19. Noor Eteram A, Al-Moubaraki Aisha H (2008) Thermodynamic study of metal corrosion and inhibitor adsorption processes in mild steel/1-methyl-4[4′(−X)-styryl pyridinium iodides/hydrochloric acid systems. Mater Chem Phys 110:145–154

20. Machnikova E, Whitmire KH, Hackerman N (2008) Corrosion inhibition of carbon steel in hydrochloric acid by furan derivatives. Electrochim Acta 53:6024–6032

21. Amar H, Tounsi A, Makayssi A, Derja A, Benzakour J, Outzourhit A (2007) Corrosion inhibition of Armco iron by 2-mercaptobenzimidazole in sodium chloride 3% media. Corros Sci 49:2936–2945

22. Avci G (2008) Corrosion inhibition of indole-3-acetic acid on mild steel in 0.5 M HCl. Colloids Surf A Physicochem Eng Aspects 317:730–736

23. Quraishi MA, Ahamad I, Singh AK, Sudhish Shukla B, Lal VakilSingh (2008) N- (Piperidinomethyl)-3-[(pyridylidene)amino] isatin: a new and effective acid corrosion inhibitor for mild steel. Mater Chem Phys 112:1035

24. Bentiss F, Traisnel M, Lagrenee M (2000) The substituted 1,3,4-oxadiazoles: a new class of corrosion inhibitors of mild steel in acidic media. Corros Sci 42:127

25. Olusegun K, Abiola OK, James AO (2010) The effects of aloe vera extract on corrosion and kinetics of corrosion process of zinc in HCl solution. Corros Sci 52:661–664